Evaluation of a hybrid capture–based pan-cancer panel for analysis of treatment stratifying oncogenic aberrations and processes

Kroeze, Leonie I.; De Voer, Richarda M.; Kamping, Eveline J.; Von Rhein, Daniel; Jansen, Erik A.m.; Hermsen, Mandy J.w.; Barberis, Massimo C.p.; Botling, Johan; Garrido-martin, Eva M.; Haller, Florian; Lacroix, Ludovic; Maes, Brigitte; Merkelbach-bruse, Sabine; Pestinger, Valerie; Pfarr, Nicole; Stenzinger, Albrecht; Van Den Heuvel, Michel M.; Grünberg, Katrien; Ligtenberg, Marjolijn J.l.

DOI:
10.1016/j.jmoldx.2020.02.009

Document Version
Publisher's PDF, also known as Version of record

Citation for published version (Harvard):
Kroeze, LI, De Voer, RM, Kamping, EJ, Von Rhein, D, Jansen, EAM, Hermsen, MJW, Barberis, MCP, Botling, J, Garrido-martin, EM, Haller, F, Lacroix, L, Maes, B, Merkelbach-bruse, S, Pestinger, V, Pfarr, N, Stenzinger, A, Van Den Heuvel, MM, Grünberg, K & Ligtenberg, MJL 2020, 'Evaluation of a hybrid capture–based pan-cancer panel for analysis of treatment stratifying oncogenic aberrations and processes', *Journal of Molecular Diagnostics*, vol. 22, no. 6, pp. 757-769. https://doi.org/10.1016/j.jmoldx.2020.02.009

The Journal of Molecular Diagnostics, Vol. 22, No. 6, June 2020

ELSEVIER

the Journal of Molecular Diagnostics
jmd.amjpathol.org

Evaluation of a Hybrid Capture–Based Pan-Cancer Panel for Analysis of Treatment Stratifying Oncogenic Aberrations and Processes

Leonie I. Kroeze,[*] Richarda M. de Voer,[†] Eveline J. Kamping,[†] Daniel von Rhein,[†] Erik A.M. Jansen,[†] Mandy J.W. Hermsen,[*] Massimo C.P. Barberis,[‡] Johan Botling,[§] Eva M. Garrido-Martin,[¶] Florian Haller,[‖] Ludovic Lacroix,[**] Brigitte Maes,[††] Sabine Merkelbach-Bruse,[‡‡] Valerie Pestinger,[§§] Nicole Pfarr,[¶¶] Albrecht Stenzinger,[‖‖] Michel M. van den Heuvel,[***] Katrien Grünberg,[*] and Marjolijn J.L. Ligtenberg[*†]

From the Departments of Pathology and Human Genetics,[†] Radboud University Medical Center, Radboud Institute for Molecular Life Sciences, Nijmegen, the Netherlands; the Division of Pathology and Laboratory Medicine,[‡] European Institute of Oncology, Milan, Italy; the Department of Immunology, Genetics and Pathology,[§] Science for Life Laboratory, Uppsala University, Uppsala, Sweden; the Instituto de Investigación i+12,[¶] University Hospital 12 de Octubre, Spanish National Center for Cancer Research and Centro de Investigación Biomédica en Red de Cáncer, Madrid, Spain; the Institute of Pathology,[‖] University Hospital Erlangen, Erlangen, Germany; the Department of Medical Biology and Pathology,[**] Institut Gustave Roussy, Villejuif, France; the Laboratory for Molecular Diagnostics,[††] Department of Clinical Biology, Jessa Hospital, Hasselt, Belgium; the Institute of Pathology,[‡‡] University Hospital Cologne, Cologne, Germany; the Institute of Cancer and Genomic Sciences,[§§] University of Birmingham, Birmingham, United Kingdom; the Institute of Pathology,[¶¶] Technical University of Munich, School of Medicine, Munich, Germany; the Institute of Pathology,[‖‖] Heidelberg University Hospital, Heidelberg, Germany; and the Department of Pulmonology,[***] Radboud University Medical Center, Nijmegen, the Netherlands*

Accepted for publication February 26, 2020.

Address correspondence to Marjolijn J.L. Ligtenberg, Ph.D., Laboratory of Tumor Genetics, Departments of Pathology and Human Genetics, Radboud University Medical Center, P. O. Box 9101, 6500 HB Nijmegen, the Netherlands.
E-mail: marjolijn.ligtenberg@radboudumc.nl.

Stratification of patients for targeted and immune-based therapies requires extensive genomic profiling that enables sensitive detection of clinically relevant variants and interrogation of biomarkers, such as tumor mutational burden (TMB) and microsatellite instability (MSI). Detection of single and multiple nucleotide variants, copy number variants, MSI, and TMB was evaluated using a commercially available next-generation sequencing panel containing 523 cancer-related genes (1.94 megabases). Analysis of formalin-fixed, paraffin-embedded tissue sections and cytologic material from 45 tumor samples showed that all previously known MSI-positive samples ($n = 7$), amplifications ($n = 9$), and pathogenic variants ($n = 59$) could be detected. TMB and MSI scores showed high intralaboratory and interlaboratory reproducibility (eight samples tested in 11 laboratories). For reliable TMB analysis, 20 ng DNA was shown to be sufficient, even for relatively poor-quality samples. A minimum of 20% neoplastic cells was required to minimize variations in TMB values induced by chromosomal instability or tumor heterogeneity. Subsequent analysis of 58 consecutive lung cancer samples in a diagnostic setting was successful and revealed sufficient somatic mutations to generate mutational signatures in 14 cases. In conclusion, the 523-gene assay can be applied for evaluation of multiple DNA-based biomarkers relevant for treatment selection. *(J Mol Diagn 2020, 22: 757–769; https://doi.org/10.1016/j.jmoldx.2020.02.009)*

With the growing number and improved efficacy of targeted therapies, and the introduction of immunotherapy, it has become increasingly evident that comprehensive tumor profiling is needed. Drugs targeting specific mutated genes or activated pathways are clinically available for several indications, and many more targeted therapies are currently

Supported by Bristol-Myers Squibb grant OT123-368 (M.J.L.L.). Part of the TruSight Oncology 500 kits were made available free of charge by Illumina.

Disclosures: Outside the submitted work, M.J.L.L. has relations with AstraZeneca, Bayer, Janssen Pharmaceuticals, Merck, and Nimagen; outside the submitted work, A.S. has relations with Bayer, Astra-Zeneca, Novartis, BMS, Seattle Genomics, Illumina, Thermo Fisher Scientific, Takeda, MSD, Pfizer, and Roche; outside the submitted work, E.M.G.-M. has been in four advisory boards for Bristol Myers Squibb, and received honoraria from Illumina; outside the submitted work, S.M.-B. has relations with AstraZeneca, Bristol Myers Squibb, Novartis, Roche, and Pfizer. Professional medical writers from Illumina wrote the introduction and *Materials and Methods* of the manuscript.

https://doi.org/10.1016/j.jmoldx.2020.02.009

being evaluated in clinical trials. In addition, in the past decade, many improvements have been made in the field of immunotherapy. Currently approved immunotherapies target the immune checkpoint proteins cytotoxic T-lymphocyte-associated protein 4 and/or programmed cell death protein 1 (PD-1) or its ligand, programmed cell death 1 ligand 1 (PD-L1). Although the introduction of immunotherapy has benefitted many patients, more than half of the patients show no clear evidence of response.[1–4] Furthermore, these therapies are expensive and can have serious adverse effects.[5–8] PD-L1 expression is an approved predictive biomarker for immunotherapy,[9] but its analysis by immunohistochemistry has several significant challenges, including the typical interobserver variability in scoring and the use of different antibodies and different staining platforms.[10–12] Moreover, it has limited predictive value as some patients with low or even negative PD-L1 expression have been shown to benefit from immunotherapy.[13,14] The first Food and Drug Administration–approved tumor type–agnostic biomarker for immunotherapy is microsatellite instability (MSI). Microsatellite instability is caused by inactivation of one of the mismatch repair genes, which results in an inability to correct DNA replication errors and leads to a high amount of neopeptides that may serve as targets for the immune system.[15,16] The incidence of MSI varies among cancers, but is overall rare in most cancer types. More recently, several studies have shown that tumor mutational burden [TMB; number of mutations/megabase (mut/Mb)] correlates with clinical outcome and the effectiveness of immune checkpoint inhibitor immunotherapies[17–22] and thus may serve as a novel biomarker. Similar to MSI, the TMB value is thought to correlate with the efficacy of immunotherapy, because mutations result in slightly modified proteins that can be recognized as neoantigens by the immune system.[23,24] The TMB threshold for successful immunotherapy may differ per tumor type.[25] For lung cancer, the threshold was set at 10 mut/Mb in the CheckMate 568.[19] Several factors are associated with an increased TMB.[26] For example, environmental factors, like UV light and tobacco use, can be responsible for an increased mutational load in melanoma and lung cancer, respectively.[27–29] Also, MSI and mutations in exonuclease domains of DNA polymerase ε (*POLE*) and DNA polymerase δ 1 (*POLD1*), involved in DNA repair, can lead to a high TMB.[29–32] In addition, the detection of mutations and amplifications associated with resistance to targeted[33,34] and immunotherapy[35] becomes increasingly important.

Because the amount of DNA available for genetic analysis is often limited, it is preferred to simultaneously assess all major genetic biomarkers and drug targets important for targeted as well as immune-based therapies, in one single assay. The current article evaluates TruSight Oncology 500 (TSO500; Illumina, San Diego, CA), a next-generation sequencing (NGS) panel containing 523 cancer-related genes (1.94 Mb) that can be used to assess pathogenic single-nucleotide variants (SNVs) and multiple-nucleotide variants, copy number variants (CNVs), MSI, and TMB. TSO500 was selected because it is a hybrid capture–based assay evaluating >1.2 Mb of coding sequence that uses unique molecular identifiers (UMIs) to enable sensitive mutation detection and to reduce the background noise that is caused by deamination artifacts in formalin-fixed materials. Detection of mutations and CNVs and the intralaboratory and interlaboratory reproducibility of TMB and MSI analyses were evaluated using different amounts and sources of input material and different neoplastic cell percentages. Finally, to evaluate the applicability of the TSO500 assay in clinical practice, a consecutive series of 58 lung cancer samples was analyzed. For samples with >30 somatic SNVs, mutational signature analysis was performed.

Materials and Methods

Sample Collection

To evaluate the performance of the TSO500 DNA assay, 45 tumor samples were selected from our routine clinical practice on the basis of known genetic defects (including samples with splice site mutations and large deletions or duplications in relevant genes), amplifications (low and high level), and MSI status. This set of tumor samples consists of samples from different tumor types: lung ($n = 16$), colon ($n = 7$), melanoma ($n = 6$), bladder ($n = 4$), endometrium ($n = 2$), ovary ($n = 2$), prostate ($n = 2$), gastrointestinal stromal tumors ($n = 2$), glioblastoma ($n = 1$), larynx ($n = 1$), pancreas ($n = 1$), and salivary gland ($n = 1$). Mean patient age was 66 years (range, 40 to 96 years). In addition, 11 normal tissue samples were used in this evaluation phase. The mean age of these individuals was 67 years (range, 49 to 72 years). One of the control samples was a peripheral blood sample, and the other 10 samples were healthy tissue from colon ($n = 3$), lung ($n = 3$), lymph node ($n = 3$), and prostate ($n = 1$). After implementation of the assay in routine diagnostics, 58 consecutive lung cancer samples were analyzed.

Most samples ($n = 87$) were formalin-fixed, paraffin-embedded (FPPE) tissue samples. In addition, one blood sample (normal control), one cerebrospinal fluid sample, one fresh frozen tissue sample, and 24 cytologic materials (16 embedded in agar, six Giemsa-stained tissue slides, and two Papanicolaou-stained slides) were used. More information about the samples used for the different analyses can be found in Figure 1 and Supplemental Table S1. The study was conducted in accordance with the institutional guidelines and regulations from Radboud University Medical Center (Nijmegen, the Netherlands; Commissie Mensgebonden Onderzoek 2018-4758).

Nucleic Acid Extraction

Genomic DNA was isolated from tissue sections (generally 6 × 10 μm) using 5% Chelex-100 and 400 μg proteinase K,

followed by purification using the QIAamp DNA Micro Kit (Qiagen, Venlo, the Netherlands). DNA concentrations were measured using the Qubit Broad Range kit (Thermo Fisher Scientific, Waltham, MA). Subsequently, 40 ng DNA was used as input for the library preparation. A DNA integrity number (DIN), a measure for the size of the DNA fragments and consequently the DNA quality, was determined using the Genomic DNA ScreenTape (Agilent Technologies, Santa Clara, CA) on an Agilent 2200 TapeStation system (Agilent Technologies). During the verification phase, it was observed that a more accurate DNA input amount could be obtained when the DNA was first diluted to 10 ng/μL using 0.1× Tris-EDTA, after which the concentration was remeasured using the Qubit High Sensitivity kit (Thermo Fisher Scientific). In addition, purification using the QIAamp DNA Micro Kit turned out not to be required. These two modifications were applied before analyzing 58 consecutive lung cancer samples in routine diagnostics.

TSO500 Library Preparation for Sequencing

Library preparation was performed using the hybrid capture–based TSO500 library preparation kit following the manufacturer's protocol. The TSO500 assay contains probes for 523 genes (Supplemental Table S2) and makes use of UMIs to analyze the number of individual DNA molecules sequenced at every position (unique coverage). Briefly, DNA was fragmented using a Covaris S2 (Covaris, Woburn, MA) to generate DNA fragments of 90 to 250 bp, with a target peak at approximately 180 bp. Samples next underwent end repair and A-tailing, before ligation of UMIs and amplification to add index sequences for sample multiplexing. Two hybridization/capture steps were performed. For the first hybridization, a pool of oligonucleotides specific to the 523 genes targeted by the TSO500 was hybridized to the prepared DNA libraries overnight. Next, streptavidin magnetic beads were used to capture probes hybridized to the DNA regions of interest. A second hybridization using the same probe set was performed to ensure high specificity of the captured regions. Next, the enriched libraries were amplified by PCR before purification using sample purification beads. Libraries were quantified and then normalized to ensure a uniform library representation. Finally, the libraries were pooled, denatured, and diluted to the appropriate loading concentration.

Sequencing and Data Analysis

Libraries were sequenced on a NextSeq 500 (Illumina), with eight to 10 libraries sequenced per run (NextSeq high output). The sequence data were processed and analyzed by the TruSight Oncology 500 Local App version 1.3 (Illumina). UMIs are used in the analysis to determine the unique coverage at each position and to reduce the background noise that is caused by sequencing and deamination artifacts in formalin-fixed material. The software produces a

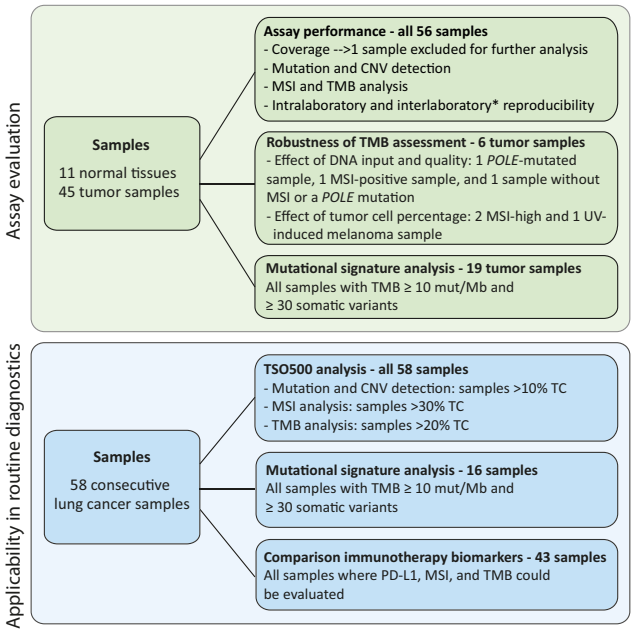

Figure 1 Study outline. In the first phase of the study, the assay performance, robustness of tumor mutational burden (TMB) assessment, and the possibility to perform mutational signature analysis were evaluated. Subsequently, the applicability of the assay in routine diagnostics was evaluated in a consecutive series of 58 lung cancer specimens that required molecular diagnostic evaluation. Laboratories indicated by the **asterisk** can be found in the author affiliations. CNV, copy number variant; MSI, microsatellite instability; mut, mutation; PD-L1, programmed cell death 1 ligand 1; TC, tumor cell percentage; TSO500, TruSight Oncology 500.

report including total and nonsynonymous mutations per Mb scores for TMB, the number and percentage of unstable sites for MSI, and quality parameters like median unique exon coverage and insert size (Supplemental Table S1). Moreover, coverage tables and a variant call file for single- and multiple-nucleotide variants, including number and percentage of variant alleles, are provided. For TMB estimation, variants are classified as somatic or germline by using bioinformatical approaches, which make use of various databases [including Catalogue of Somatic Mutations in Cancer (COSMIC), The Genome Aggregation Database (gnomAD), and 1000 genomes project] and take into account the variant allele frequencies (VAFs) of surrounding germline variants. For TMB calculation, somatic SNVs with a VAF >5% are included. Hotspot mutations are excluded to avoid overestimation of TMB, because the gene panel is biased toward frequently mutated genomic regions (cancer-related genes).

An in-house developed user interface was used for variant annotation, variant filtering, and data visualization.[36] Variants were filtered by excluding the following: i) variants not overlapping with exons and splice site regions (−8/+8), ii) synonymous variants, unless located in a splice site region, and iii) variants present with a frequency >0.1% in the control population represented in The Exome Aggregation

Consortium (ExAC) version 0.2. For tailored reporting purposes, virtual gene panels were defined per tumor type in close collaboration with the clinicians. For lung cancer, a panel of 15 genes was composed (Supplemental Table S3). After filtering, all remaining variants in the gene panel were manually inspected and curated. A laboratory-developed bioinformatic pipeline was used to analyze the unique coverage and the presence of amplifications, as described previously.[37] For analyses of gene amplifications, the coverage of each region in the tumor sample was normalized using the median sequencing depth of all regions in the sample. Subsequently, a relative coverage score was calculated by dividing the normalized coverage of each region through the mean normalized coverage of this same region in a set of 11 normal control samples.

Evaluation of the Assay Performance

By analyzing formalin-fixed, paraffin-embedded and cytologic samples from our routine clinical practice, the performance of the TSO500 assay for TMB measurement, MSI analysis, variant calling, and CNV detection was determined. *POLE*-mutated and MSI-positive samples were used as positive controls, whereas normal tissue samples were used as negative controls for TMB analysis. Mutation detection, CNV analysis, and MSI analysis were evaluated by comparing the TSO500 results with results from our routine diagnostic tests. For mutation detection and CNV analysis, single-molecule molecular inversion probe (smMIP)−based NGS is used,[37−39] and for MSI detection, genescan fragment length analyses of five mononucleotide markers (pentaplex PCR), immunohistochemistry of the mismatch repair genes, and/or evaluation of 55 microsatellite markers by smMIP-based NGS using mSINGS software version 3.4 are used.[39,40]

The intralaboratory reproducibility of TMB and MSI measurements was determined through analysis of the same commercially available control sample, obtained from Horizon Dx (Cambridge, UK), in 10 runs. For multisite reproducibility studies, a control panel of eight DNA samples was sent to 11 independent laboratories, consisting of DNA derived from six cell lines, one formalin-fixed, paraffin-embedded tissue sample, and the Horizon Dx control.

To further assess the performance and robustness of TMB analysis, TMB values were measured and compared under different conditions. First, dilution series were performed to determine the minimal amount of input DNA to reliably measure TMB. In addition, DNA quality (using DIN scores) was correlated with median exon coverage to determine a minimal quality value for reliable variant calling and TMB analysis. Dilution series made by mixing tumor DNA with normal DNA from the same patient (to mimic different percentages of neoplastic cells) were used to determine the minimal tumor cell percentage.

Mutational Signature Analysis

To infer the contribution of the 49 mutational signatures available at COSMIC (Mutational Signatures version 3, *https://cancer.sanger.ac.uk/cosmic/signatures/SBS/*, last accessed December 2, 2019), all samples with a nonsynonymous TMB >10 mut/Mb were selected. Next, all somatic synonymous, nonsynonymous, and intronic SNVs with a VAF >5% that were absent or reported in gnomAD three or fewer times from each sample were extracted. Synonymous and intronic variants were included in mutational signature analysis (but not in nonsynonymous TMB) to increase the number of mutations, which makes the signature analysis more reliable. Samples that harbored <30 SNVs were excluded for further analysis. For each sample, the mutation spectrum, based on all 96 trinucleotide substitutions, and the estimated contribution of each signature to the mutation spectrum were determined using the R package DeconstructSigs.[41]

Results

Assay Performance and Reproducibility

The performance of the TSO500 assay was evaluated using DNA from 45 previously tested tumor samples and 11 normal tissue controls (Figure 1). One sample, an 8-year−old tissue block, had a median unique exon coverage of 40, which was below the predefined quality criterion of a median unique exon coverage of ≥150, which is considered essential for reliable calling of variants with a VAF of >5% (on average, 7.5 unique reads containing the variant). This sample was excluded for further analysis. For the remaining 55 samples, the median unique exon coverage, determined using UMIs, was 362 (range, 150 to 756) (Supplemental Table S1). The median nonunique coverage was 1501 (range, 844 to 2114). The coverage of all individual target regions was rather uniform; the median unique coverage of all autosomal targets varied up to one order of magnitude (Figure 2A).

All pathogenic somatic mutations (n = 59) detected using our routine diagnostics smMIP-based NGS analysis[38,39] were also detected by the TSO500 assay (Figure 2B and Supplemental Table S4). Two deliberately selected exceptionally complex variants, a deletion of 45 nucleotides and a duplication of 48 nucleotides in *KIT* (Supplemental Table S4), were not called by the pipeline but were clearly present in the data (Supplemental Figure S1). Other large insertions/deletions were correctly called, including a 30-nucleotide deletion in *TP53* and a 26-nucleotide deletion in *MET*. All known amplifications could be detected using the TSO500 assay (Figure 2C and Supplemental Table S5). All seven MSI-positive samples had >30% (median, 64%; range, 34% to 80%) unstable microsatellite (MS) sites, whereas all negative samples had <20% unstable MS sites (median, 7%; range, 0% to 16%) (Figure 2D and

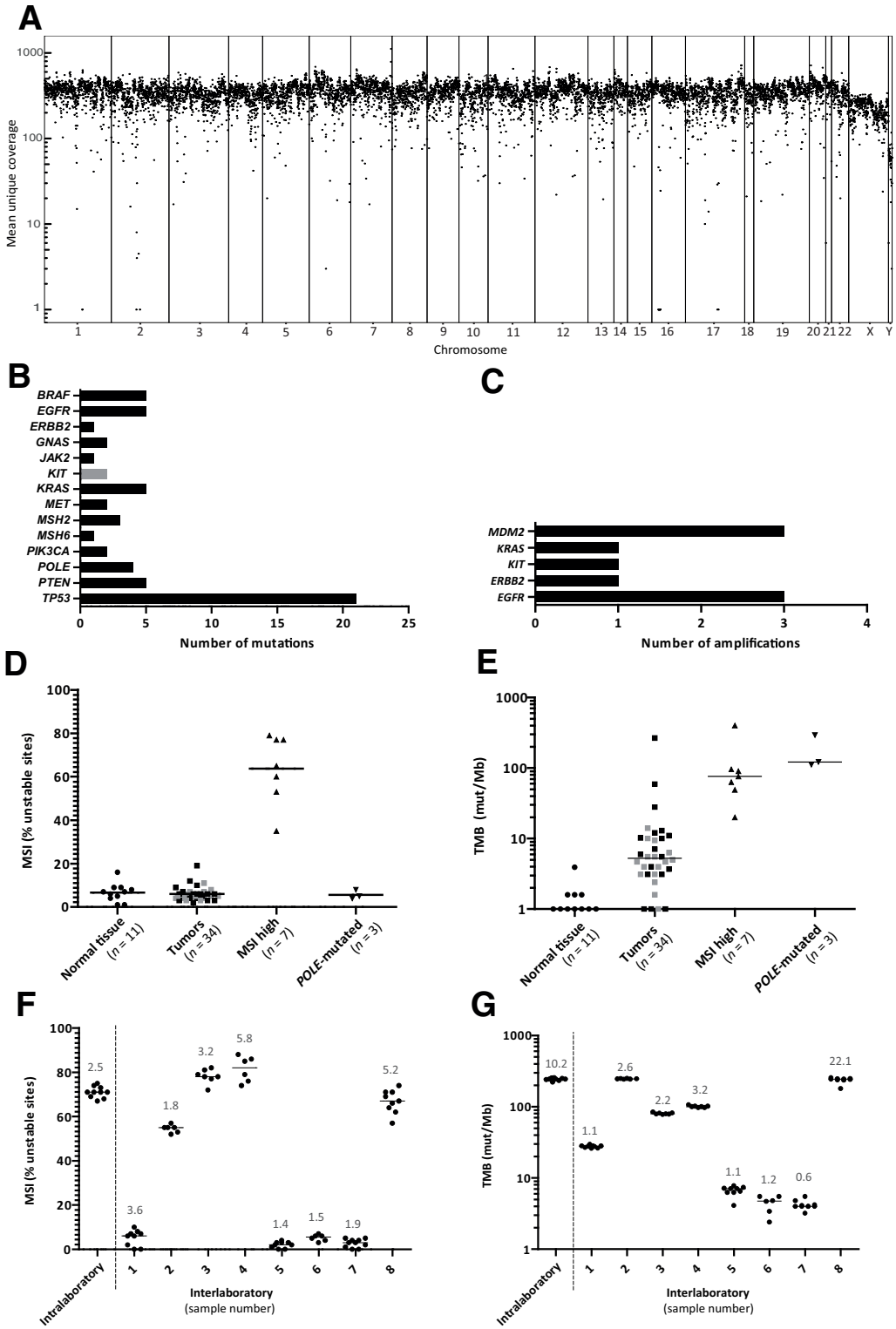

Figure 2 Assay performance. **A:** Uniform unique coverage of TruSight Oncology 500 (TSO500) target regions (mean of 55 samples). Target regions are plotted per chromosomal position. **B:** Known pathogenic mutations were all detected using the TSO500 assay. Two complex *KIT* mutations were not called by the software (marked in gray). **C:** Known copy number variants were all detected using TSO500. **D:** All seven microsatellite instability (MSI)—positive samples showed a percentage of unstable microsatellite (MS) sites >30%, whereas all negative samples had <20% unstable MS sites. Lung tumors are indicated in gray. **E:** MSI-positive and *POLE*-mutated samples showed a high tumor mutational burden (TMB). In the other tumor samples, a wide range of TMB values could be observed. Lung tumors are indicated in gray. **F** and **G:** TMB and MSI values of a set of control samples showed extremely good reproducibility, both intralaboratory and interlaboratory. Control samples with <150× median unique exon coverage were excluded. The SD is indicated above each sample. The **dotted line** separates intralaboratory reproducibility results (**left side**) from interlaboratory reproducibility results (**right side**). $n = 59$ (**B**); $n = 9$ (**C**); $n = 11$ laboratories (**F** and **G**). Mut, mutation.

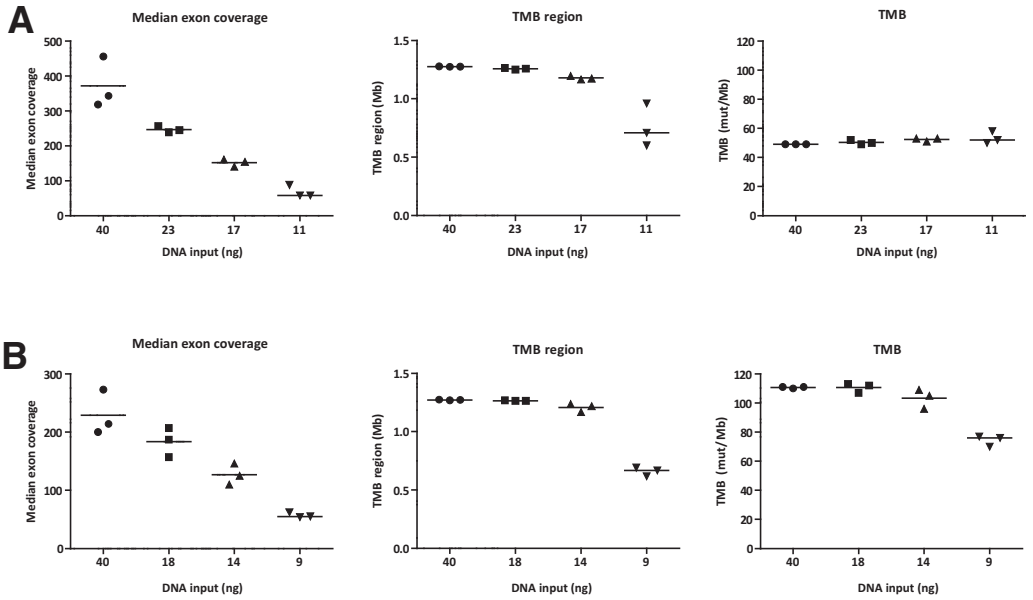

Figure 3 Effect of DNA input amount on tumor mutational burden (TMB) analysis. **A** and **B:** Two samples were analyzed with different DNA input amounts (in triplicate). A positive correlation was observed between the DNA input amount and median unique exon coverage, and consequently the region sufficiently covered for TMB analysis (>50 unique reads). **A:** Microsatellite instability–positive sample [unique patient number (UPN) 39] with 80% tumor cells [DNA integrity number (DIN) score, 4.2]: TMB analysis remains stable even with 11 ng DNA input. **B:** *POLE*-mutated sample (UPN40) with 30% tumor cells (DIN score, 2.5): TMB analysis remains more or less stable down to 14 ng, and starts to decrease with less DNA input. Mut, mutation.

Supplemental Table S1). Of note, one sample with an intermediate level of microsatellite instability using pentaplex PCR analyses of five mononucleotide markers and evaluation of smMIP-based NGS using 55 MS markers showed 34% unstable MS sites with the TSO500 analysis. The decision was made to use the following criteria for diagnostic evaluations: samples with ≥30% unstable microsatellites are classified as MSI positive; samples with <15% unstable microsatellite loci are classified as MS stable; and for samples with 15% to 30% unstable microsatellites, immunohistochemistry of mismatch repair proteins and/or pentaplex PCR will be used to clarify the MSI status.

To evaluate TMB analysis, all 55 samples, representing 11 normal tissue samples, seven MSI-positive tumors, three

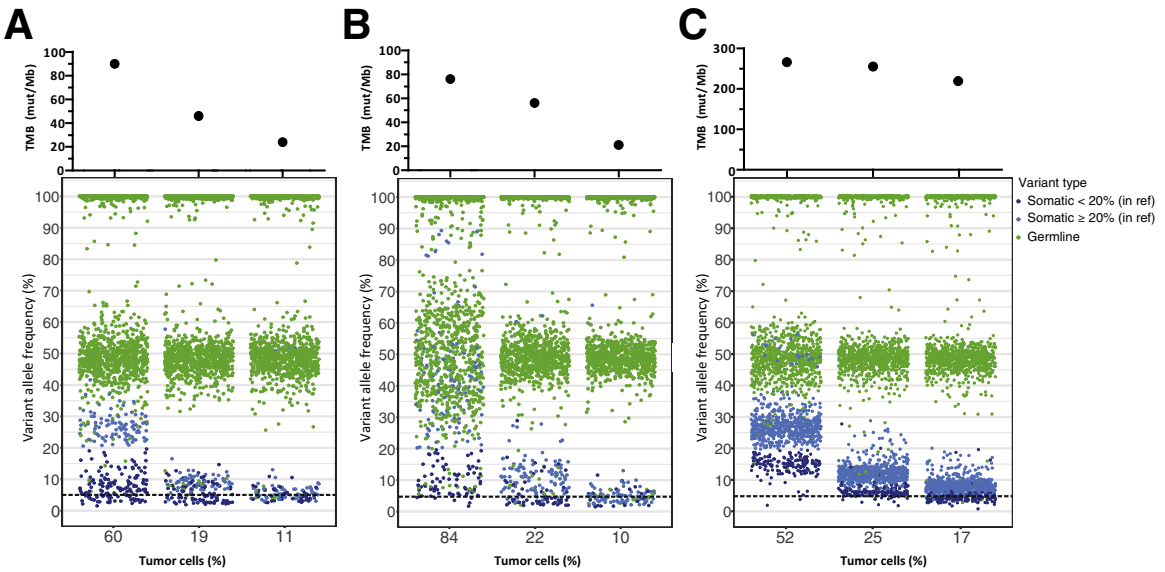

Figure 4 Effect of tumor cell percentage on tumor mutational burden (TMB) analysis. **A**–**C:** Three TMB-high tumor samples were diluted with normal tissue of the same patient, to mimic decreasing tumor cell percentages. Germline variants are indicated in green. Predicted somatic variants are shown in blue, with dark blue indicating variants with a variant allele frequency (VAF) ≥20%, and light blue indicating variants with a VAF <20% in the original tumor sample. **A** and **B:** Two microsatellite instability–positive samples [unique patient number (UPN) 37 (**A**) and UPN27 (**B**)] showed a clear decrease in TMB values, due to the wide range of VAFs caused by a deficiency in DNA repair. **C:** UV-induced melanoma sample (UPN51) with a rather stable TMB. Two groups of somatic variants can be distinguished, likely caused by chromosomal instability. **Dotted line** indicates VAF threshold for TMB analysis. Ref, reference.

tumors with a *POLE* mutation, and 34 tumor samples without MSI or a *POLE* mutation (16 lung cancer samples and 18 samples of other tumor types) (Figure 2E and Supplemental Table S1) were analyzed using the accompanying software. On average, per sample, 78% of detected somatic mutations were nonsynonymous. The correlation between total TMB (including synonymous and nonsynonymous variants) and nonsynonymous TMB was strong ($R = 0.994$) (Supplemental Figure S2). Nonsynonymous TMB values (mut/Mb) are further used in this study and referred to as TMB. Sequencing of normal tissue samples revealed a low background TMB value (median, 1 mut/Mb; range, 0 to 3.9 mut/Mb). MSI-positive samples (median, 76 mut/Mb; range, 20 to 402 mut/Mb) and samples with a *POLE* mutation (median, 122 mut/Mb; range, 111 to 292 mut/Mb) had consistently high TMB values. In the other 34 tumor samples, a wide range of TMB values was observed (median, 5.5 mut/Mb; range, 0 to 266 mut/Mb). The three outlier high TMB values in this group were two melanoma and one bladder cancer sample.

Intralaboratory reproducibility of the assay was assessed using a control sample that was included in 10 sequencing runs. Both MSI and TMB values were reproducible (MSI: median, 71% unstable sites; SD, 3%; TMB: median, 245 mut/Mb; SD, 9.8 mut/Mb) (Figure 2, F and G). Interlaboratory reproducibility was assessed by analyzing eight samples at 11 independent laboratories. The MSI and TMB results were consistent (Figure 2, F and G), indicating that the assay is robust and the data analysis is highly reproducible.

DNA Quantity, DNA Quality, and Tumor Cell Percentage May Influence TMB Assessment

Subsequently, it was analyzed whether the DNA quality and quantity can affect the TMB value. A positive correlation was observed for both DNA quality and DNA input amount with median unique exon coverage (both $P < 0.0001$) (Supplemental Figure S3). To test whether DNA quality and quantity affect TMB analysis, one high-quality (DIN, 4.2) sample and one low-quality (DIN, 2.5) sample with a high TMB were analyzed using different DNA input amounts (in triplicate). The high DNA quality sample, an MSI-positive sample with 80% tumor cells, showed highly reproducible TMB values, even at the lowest tested DNA input amount (11 ng) (Figure 3A). The low DNA quality sample, a *POLE*-mutated sample with 30% tumor cells, showed stable TMB results at DNA inputs of 40, 18, and 14 ng (Figure 3B). However, at the lowest tested DNA input amount (9 ng), the median exon coverage decreased to 57, which was accompanied by a decrease in TMB value. A similar DNA input range was performed using sample UPN49 with a TMB of 10.2 mut/Mb (70% tumor cells and a low DNA quality: DIN, 2.1), which showed stable TMB results using 40 and 20 ng DNA input and a little deviation when using 15 and 10 ng because of a decrease in the region that was taking into account for TMB calculation (Supplemental Figure S4). In conclusion, these experiments indicate that 20 ng of DNA, an equivalent of 3000 cells, seems to be sufficient for reliable TMB measurement, even in samples with a rather poor DNA quality. This amount is available for the vast majority of clinical specimens, even in case of small biopsies or cytologic samples. Of note, when using low DNA input amounts, the median unique exon coverage decreases below the threshold of 150, whereas the median nonunique exon coverage is still high (>900×), indicating the presence of many duplicate reads. This highlights the importance of using UMIs to prevent overinterpreting the sequencing data.

To determine the minimal tumor cell percentage to reliably measure TMB, a dilution series was performed using three samples with a high TMB and the matched normal DNA from these patients (Figure 4). The tumor cell percentages of the original samples were estimated by a pathologist. After sequencing, the actual tumor cell percentages of the original samples and subsequent dilutions were determined using VAFs of three different mutations (Supplemental Figure S5). When decreasing the tumor cell percentage, the VAFs of all somatic variants will decrease. However, as long as all variants (mut) still have a VAF above the cutoff of 5% (as used in the TMB analysis software) and the panel size is equal (Mb), the TMB (mut/Mb) will stay the same. Of interest, with decreasing tumor cell percentages, a marked decrease in TMB in two MSI-positive samples was observed (Figure 4, A and B). The VAFs of the somatic variants in these samples are heterogeneous, probably because of the underlying deficiency in DNA repair (Supplemental Figure S6). When the tumor cell percentage decreases, the VAF of some of these somatic variants decreases below the cutoff of 5% used in the TMB analysis software, leading to a decrease in TMB value. In a melanoma sample with high TMB due to UV-induced damage (as verified by its mutational signature; see below), the TMB value remained stable in samples with 52% and 25% tumor cells (Figure 4C), but a slight decrease in TMB was observed at 17% tumor cells. This decrease in TMB is likely caused by chromosomal instability (Supplemental Figure S6). When one of the chromosomes of a chromosome pair is duplicated, the variants on the noncopied chromosome will have a lower VAF than variants on the copied chromosome and variants on chromosome pairs not affected by instability. Consequently, these variants more easily decrease below a VAF of 5% when decreasing the tumor cell percentage. Therefore, in samples with chromosomal instability, a tumor cell percentage of at least 20% seems to be required (Supplemental Figure S7). In the two samples with a defect in DNA repair (Figure 4, A and B), 20% tumor cells still result in high TMB values (>40 mut/Mb). Therefore, it is concluded that a tumor cell percentage of at least 20% is required to minimize variations in TMB values induced by chromosomal instability or tumor heterogeneity.

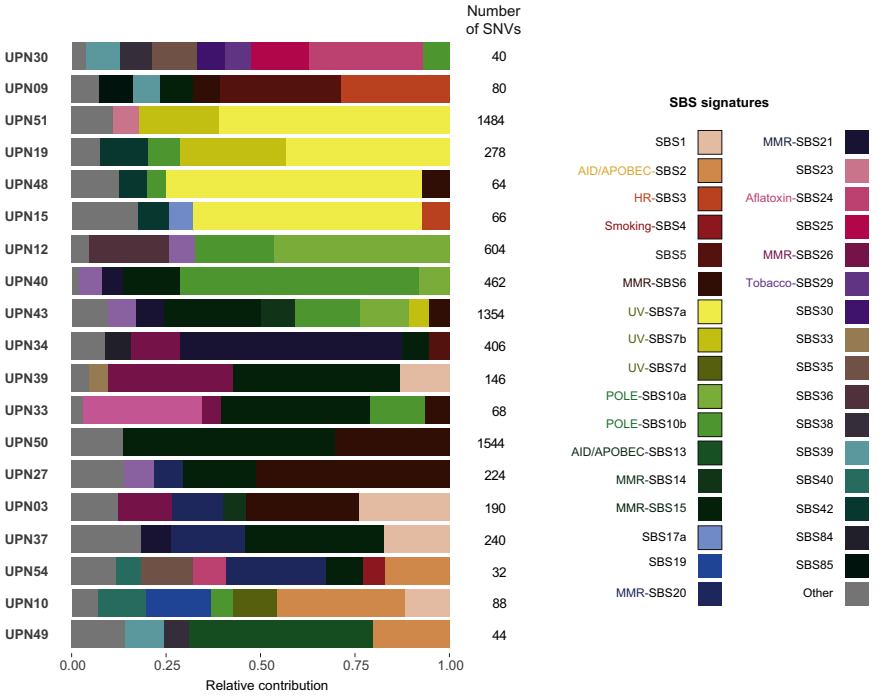

Figure 5 Mutational signature analysis. The estimated relative contribution of the 49 Catalogue of Somatic Mutations in Cancer (COSMIC) version 3 mutational signatures to the mutation spectrum of each indicated tumor sample after refitting. Signatures with a relative contribution of <0.05 are merged and marked in gray (other). The number of single-nucleotide variants (SNVs) used for the analysis is indicated for each sample. AID/APOBEC, activation induced deaminase/apolipoprotein B mRNA editing enzyme, catalytic polypeptide-like; HR, homologous recombination; MMR, mismatch repair deficiency; SBS, single-base substitution; UPN, unique patient number.

Mutational Signature Analysis

In samples with sufficient somatic mutations, refitting of predefined mutational signatures can be performed. This analysis can lead to additional information regarding the mutational processes involved in tumorigenesis. For samples with a high TMB (>10 mut/Mb) and ≥30 somatic SNVs ($n = 19$), mutational signature analysis based on refitting was performed. In 95% of these samples (18/19), the observed mutation spectrum highly resembled one or

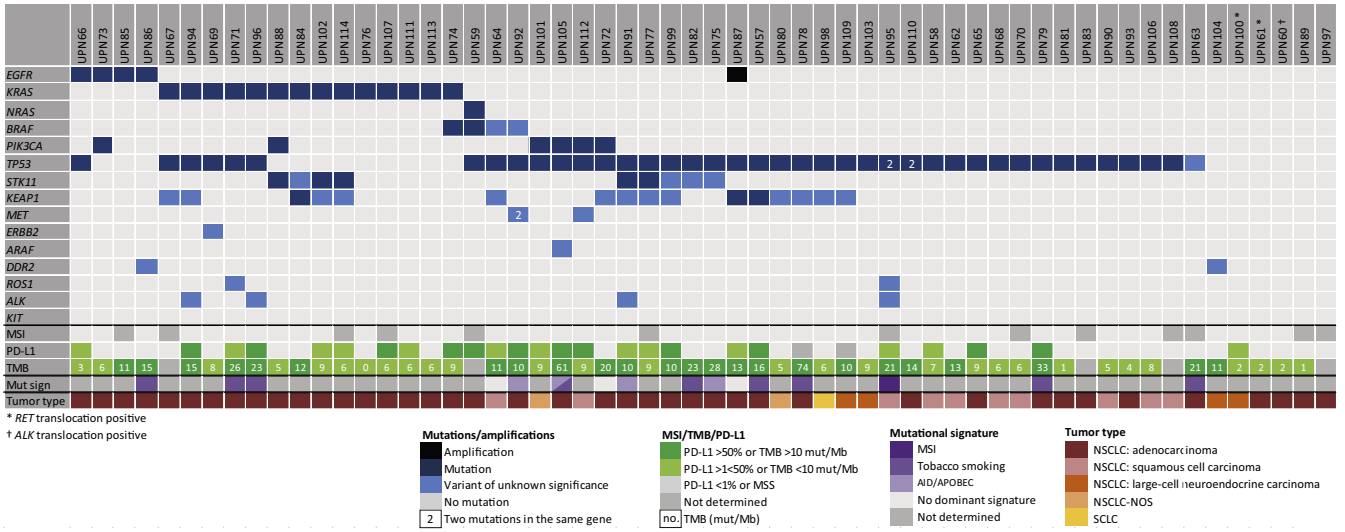

Figure 6 Results of TruSight Oncology 500 (TSO500) lung cancer requests. Mutations (dark blue) and variants of unknown significance (light blue) detected in our TSO500 lung cancer panel (15 genes) are shown per patient. In addition, microsatellite instability (MSI), tumor mutational burden (TMB), PD-L1 status, and tumor type are indicated. Only samples with a sufficient tumor cell percentage were analyzed for MSI (≥30% tumor cells) and TMB (≥20% tumor cells). The number of mutations per Mb is indicated. For samples with ≥30 somatic variants, mutational signature analysis was performed. Signatures with a high contribution to the mutational pattern are indicated (purple colors). Patients are grouped based on mutated gene(s). The **asterisk** indicates *RET* translocation positive; and the **dagger**, *ALK* translocation positive. AID/APOBEC, activation induced deaminase/apolipoprotein B mRNA editing enzyme, catalytic polypeptide-like; Mut sign, mutational signature; NOS, not otherwise specified; NSCLC, non-SCLC; PD-L1, programmed cell death 1 ligand 1; SCLC, small-cell lung cancer; UPN, unique patient number.

more main mutational processes (Figure 5). After refitting of the mutation spectrum of each sample to the 49 described mutational signatures, signatures 10a and 10b, known to be associated with *POLE* mutations, emerged as the main mutational process in the three samples with a pathogenic somatic mutation in the exonuclease domain of *POLE* (UPN12, UPN40, and UPN43) (Figure 5 and Supplemental Figure S8A). Moreover, the signatures for UPN43 indicated an additional role for mismatch repair deficiency (Figure 5 and Supplemental Figure S8C). In all seven MSI-positive tumors, the mutation spectrum can primarily be explained by signatures that are associated with microsatellite instability (signatures 6, 15, 20, 21, and 26) (Figure 5 and Supplemental Figure S8B). In four other samples, including the two samples with the highest TMB without MSI or a pathogenic *POLE* mutation (UPN19: 56 mut/Mb; and UPN51: 266 mut/Mb) (Figure 2E), the mutation spectrum showed a high contribution of signature 7, indicating exposure to UV light as the main mutational process in these tumors (Figure 5 and Supplemental Figure S8D). All four tumors were melanomas.

In two samples (UPN50 and UPN51), a variant in the *POLE* exonuclease domain (p.Val411Met and p.Pro418Ser) was identified. No literature is available that proves the pathogenicity of these variants. The valine on position 411 is a well-known hotspot location for *POLE* mutations that lead to a POLE signature; however, in UPN50, the valine is substituted by a methionine, whereas the known pathogenic mutation is a substitution by leucine. Although the TMB in both samples was extremely high (UPN50: 402 mut/Mb; and UPN51: 266 mut/Mb), refitting of the mutational signatures did not show a main contribution of *POLE* to the mutational process, suggesting that most of the mutations are caused by other mechanisms (UV exposure in UPN51 and MSI in UPN50) (Figure 5). This indicates that both *POLE* mutations may be passenger mutations or late pathogenic events that barely contributed to the mutational signature in these samples.

Comprehensive Analysis of a Consecutive Series of Lung Tumors

To evaluate the applicability of the TSO500 assay in clinical practice, a consecutive series of 58 lung tumor samples received for diagnostic evaluation was tested (Supplemental Table S6). All cytologic samples ($n = 18$), tissue biopsies ($n = 21$), and surgical resections ($n = 19$) were sequenced successfully. Detailed evaluation of somatic mutations was performed for a panel of 15 genes (Supplemental Table S3) that are commonly mutated in lung cancer and/or potentially actionable. One or more mutations were detected within these genes in 91% of the tumors (Figure 6 and Supplemental Table S6). The most frequently mutated gene was *TP53* (69%), followed by *KEAP1* (28%), *KRAS* (24%), and *STK11* (16%). *EGFR* (7%) and *KRAS* mutations were exclusively found in adenocarcinoma samples. Because the full coding region of each gene is covered, it was also possible to detect potentially clinically relevant mutations in regions of *BRAF* (p.Glu501Gly) and *PIK3CA* (p.Arg88Gln, p.Arg93Trp, p.Lys111Asn, and p.Gly118Asp) that are not frequently mutated, and therefore not present in most commercially available targeted NGS panels. In patient UPN73, who previously tested positive for an activating *EGFR* mutation, leading to treatment with erlotinib followed by osimertinib, a less common *PIK3CA* mutation (p.Gly118Asp) could most likely explain the acquired EGFR tyrosine kinase inhibitor resistance. *ALK*, *ROS1*, and *RET* translocations were assessed using standard immunohistochemistry and/or fluorescence *in situ* hybridization techniques. One *ALK* and two *RET* translocations were detected in this cohort (Figure 6).

The most effective cutoff for a high TMB is still under investigation in clinical trials, but is set at 10 mut/Mb for lung cancer in the Checkmate 568.[19] When applying this threshold, 45% of the samples had a high TMB. Refitting of the mutational signatures of all samples with $\geq$30 somatic mutations ($n = 16$) revealed nine samples (56%) with a large contribution of signature 4, which is highly associated with tobacco smoking (Figure 6 and Supplemental Figure S9). Four samples with a high TMB showed that the mutation spectrum was in part explained by mutational signatures associated with increased activity of the activation induced deaminase/apolipoprotein B mRNA editing enzyme, catalytic polypeptide-like (AID/APOBEC) family of cytidine deaminases (signatures 2 and 13) (Figure 6 and Supplemental Figure S9). Of interest, although none of the investigated lung cancer samples in this diagnostic series showed MSI according to TSO500 analysis, refitting of the mutation spectrum of UPN95 showed relatively high contribution of signature 6, which is associated with mismatch repair deficiency (Supplemental Figure S9). This sample did not meet our minimum acceptance criteria of $\geq$30% tumor cells for reliable MSI analysis (25% tumor cells and 10% unstable MS sites) (Supplemental Table S6). Subsequent analysis of another sample of this tumor, containing 50% tumor cells, resulted in 22% unstable MS sites. Indeed, smMIP-based NGS analysis and pentaplex PCR both confirmed a (subtle) unstable pattern.

PD-L1 positivity [antibody 22C3 pharmDx (Agilent Technologies) or E1L3N (Cell Signaling Technology, Danvers, MA)] was detected in 43% of the samples. No correlation could be observed between PD-L1 positivity and a high TMB ($P = 0.2276$) (Supplemental Figure S10), indicating that these markers are independent.

Discussion

To assess whether multiple biomarkers can be determined in a single assay and to what extent different parameters may influence TMB values, a commercially available 523-gene panel, TSO500, and its accompanying software were

evaluated. DNA isolated from a range of sample types (formalin-fixed, paraffin-embedded tissue blocks, cytologic material embedded in agar, and cytologic material stained with Giemsa or Papanicolaou) was successfully sequenced. All previously determined mutations, amplifications, and MSI present in these samples were detected, although two exceptionally large insertions/deletions required visual inspection of the aligned reads. CNV detection is increasingly becoming integrated in NGS panels.[37] An advantage of using TSO500 for CNV detection is that all genes are completely covered, which makes CNV detection more reliable compared with NGS panels in which only a few regions of a gene are analyzed.

The TSO500 is able to determine TMB values without the need for matched normal DNA by using bioinformatic approaches to discriminate between germline and somatic variants. This a major advantage because obtaining and sequencing DNA from normal tissue is not always feasible, is rather expensive, and may lead to ethical issues concerning the risk to detect pathogenic germline variants. On the other hand, by using this bioinformatic approach, some variants may be incorrectly labeled as germline or somatic, which might slightly affect the TMB value. During assay evaluation, TMB values were observed to be uniformly low in normal tissue samples and high in samples with MSI or a *POLE* mutation. High interlaboratory reproducibility in MSI and TMB values was shown. Furthermore, a recent publication shows good agreement between TSO500 and whole exome sequencing–based TMB assessment.[42] These results demonstrate that the assay performs well, even without using matched normal DNA.

As TMB is an emerging biomarker for stratification of patients for immunotherapy, it is essential to understand the reliability of the TMB values assessed under different conditions. Recent publications highlight the importance of panel size, panel content, and bioinformatic parameters for reliable panel-based TMB estimation.[29,43–45] No comprehensive experiments have been performed thus far to determine the effect of DNA quality, DNA quantity, and tumor cell percentage on TMB assessment. The analyses in this manuscript show that both a low DNA input amount and poor DNA quality can lead to a decrease in the median unique exon coverage and consequently the measured TMB value. On the basis of the findings presented herein, 20 ng of DNA is considered to be sufficient for reliable TMB evaluation, even in relatively poor-quality samples. Sufficient coverage (median unique exon coverage of $\geq$150) could be obtained for all DNA samples with a DIN score >2. Furthermore, the TMB value may be influenced by the tumor cell percentage in heterogeneous tumors (eg, MSI-positive tumors) and tumors with a high degree of chromosomal instability. The TMB in heterogeneous tumors may also differ depending on the site where the biopsy is taken, as described by Kazdal et al.[42] Overall, it is concluded that for TSO500 analyses, a tumor cell percentage of $\geq$20% is required for TMB analysis, because at 20% tumor cells, somatic mutations on the noncopied chromosome in samples with chromosomal instability (up to four chromosome copies) still have a VAF >5% (Supplemental Figure S7), and samples with defects in DNA repair (Figure 4, A and B) still have high TMB values (>40 mut/Mb).

A benefit of using a large gene panel is that mutational signature analysis can be performed in samples with sufficient mutations. In most samples with $\geq$30 presumed somatic SNVs, a mutational signature could be defined that matched with the known underlying mutational mechanism (eg, DNA mismatch repair deficiency or hypermutation due to a *POLE* mutation) or corresponded with the tissue of origin (UV signature in melanoma samples or tobacco smoking in lung cancer). More importantly, these mutational signatures may support the differential diagnosis in cases of metastasis of unknown primary origin, allow the classification of potential pathogenic variants in DNA repair genes, and may determine the presence of mutational processes important for tumorigenesis and therapy choice that are not supported by specific somatic variants, but are, for example, caused by promoter hypermethylation.[46]

After evaluation of the assay performance, the applicability of the assay in daily practice was confirmed in a consecutive series of 58 lung cancer specimens that required molecular diagnostic evaluation. The frequency of detected genetic aberrations in the investigated cohort might slightly differ compared with other cohorts because this is a mixed cohort of adenocarcinoma and squamous cell carcinoma samples, which also contains stage I and II non–small-cell lung cancer patients. In addition, a selected population of lung cancer patients from surrounding hospitals is referred to our center, leading to some bias in this cohort. In the tested cohort, a TMB $\geq$10 mut/Mb was found in 45% of the lung cancer samples, which is consistent with previous reports.[19] Refitting of the mutational signatures revealed that more than half (9/16) of these TMB-high samples showed a mutational signature associated with smoking. In addition, four TMB-high samples showed mutational signatures associated with increased activity of the AID/APOBEC protein family. These proteins play an important role in mRNA editing by deaminating cytosines; however, when misregulated, this may result in multiple mutations.[47] Recent studies showed that non–small-cell lung cancer patients with a high TMB associated with an AID/APOBEC mutational signature showed a strong correlation with response to immunotherapy.[48,49] Finally, in one biopsy sample, the mutation spectrum showed high similarity with signature 6. Of interest, the MSI status in this sample could not be determined because the tumor cell percentage (25%) was below the predefined cutoff of $\geq$30%. The result of this mutational signature analysis motivated us to sequence a resection sample of this patient containing 50% tumor cells, which confirmed an intermediate level of microsatellite instability (22% unstable MS sites) and thereby highlights the added value of performing mutational signature analyses. In line with previous reports, no correlation was

observed between PD-L1 positivity and a high TMB.[19,32,50] As more studies emerge demonstrating that PD-L1, MSI, and TMB are all important markers to predict response to immunotherapy in lung cancer, it is becoming increasingly important to screen for all three biomarkers.[19,50–52]

In conclusion, the use of a large pan-cancer panel, like TSO500, allows comprehensive and simultaneous assessment of SNVs, multiple-nucleotide variants, CNVs, TMB, and MSI in a single assay. Additional benefits of using a large gene panel are that both accepted and emerging biomarkers can be measured and that mutational signatures can be determined in tumors with a sufficient number of mutations. The current article shows that for reliable TMB evaluation, it is important to consider DNA quality, DNA quantity, and the tumor cell percentage of a sample. A low DNA input amount and/or quality can result in a low median unique exon coverage, which can affect the TMB estimation. In samples with a low tumor cell percentage (<20%) that harbor many subclonal mutations or show a high level of genetic heterogeneity, TMB values may be underestimated because the frequency of some variants is below the VAF threshold of 5% and consequently these variants are not included in the TMB calculation. We, therefore, recommend that evaluations of assays for TMB assessment include a definition of minimum acceptance criteria for DNA quality, DNA quantity, and tumor cell percentage next to analysis of the reproducibility and correlation with TMB values of other assays. Only after rigorous evaluation of the used assay, TMB values can be considered as a putative biomarker for immunotherapy stratification.

Acknowledgments

We thank Monique Goossens and Annemiek Kastner-van Raaij for support with sample collection and data analysis; Steven Castelein and Christian Gilissen for bioinformatical assistance; and Rodney Moore and Kirsten Curnow, professional medical writers from Illumina, for assistance with writing the introduction and *Materials and Methods* of the manuscript.

Supplemental Data

Supplemental material for this article can be found at *https://doi.org/10.1016/j.jmoldx.2020.02.009*.

References

1. Borghaei H, Paz-Ares L, Horn L, Spigel DR, Steins M, Ready NE, Chow LQ, Vokes EE, Felip E, Holgado E, Barlesi F, Kohlhaufl M, Arrieta O, Burgio MA, Fayette J, Lena H, Poddubskaya E, Gerber DE, Gettinger SN, Rudin CM, Rizvi N, Crino L, Blumenschein GR Jr, Antonia SJ, Dorange C, Harbison CT, Graf Finckenstein F, Brahmer JR: Nivolumab versus docetaxel in advanced nonsquamous non-small-cell lung cancer. N Engl J Med 2015, 373:1627–1639
2. Chung HC, Ros W, Delord JP, Perets R, Italiano A, Shapira-Frommer R, Manzuk L, Piha-Paul SA, Xu L, Zeigenfuss S, Pruitt SK, Leary A: Efficacy and safety of pembrolizumab in previously treated advanced cervical cancer: results from the phase II KEYNOTE-158 study. J Clin Oncol 2019, 37:1470–1478
3. Gangadhar TC, Hwu WJ, Postow MA, Hamid O, Daud A, Dronca R, Joseph R, O'Day SJ, Hodi FS, Pavlick AC, Kluger H, Oxborough RP, Yang A, Gazdoiu M, Kush DA, Ebbinghaus S, Salama AKS: Efficacy and safety of pembrolizumab in patients enrolled in KEYNOTE-030 in the United States: an expanded access program. J Immunother 2017, 40:334–340
4. Kowanetz M, Zou W, Gettinger SN, Koeppen H, Kockx M, Schmid P, Kadel EE 3rd, Wistuba I, Chaft J, Rizvi NA, Spigel DR, Spira A, Hirsch FR, Cohen V, Smith D, Boyd Z, Miley N, Flynn S, Leveque V, Shames DS, Ballinger M, Mocci S, Shankar G, Funke R, Hampton G, Sandler A, Amler L, Mellman I, Chen DS, Hegde PS: Differential regulation of PD-L1 expression by immune and tumor cells in NSCLC and the response to treatment with atezolizumab (anti-PD-L1). Proc Natl Acad Sci U S A 2018, 115:E10119–E10126
5. Abdel-Wahab N, Shah M, Suarez-Almazor ME: Adverse events associated with immune checkpoint blockade in patients with cancer: a systematic review of case reports. PLoS One 2016, 11:e0160221
6. Huang Y, Fan H, Li N, Du J: Risk of immune-related pneumonitis for PD1/PD-L1 inhibitors: systematic review and network meta-analysis. Cancer Med 2019, 8:2664–2674
7. Larkin J, Chmielowski B, Lao CD, Hodi FS, Sharfman W, Weber J, Suijkerbuijk KPM, Azevedo S, Li H, Reshef D, Avila A, Reardon DA: Neurologic serious adverse events associated with nivolumab plus ipilimumab or nivolumab alone in advanced melanoma, including a case series of encephalitis. Oncologist 2017, 22:709–718
8. Schadendorf D, Wolchok JD, Hodi FS, Chiarion-Sileni V, Gonzalez R, Rutkowski P, Grob JJ, Cowey CL, Lao CD, Chesney J, Robert C, Grossmann K, McDermott D, Walker D, Bhore R, Larkin J, Postow MA: Efficacy and safety outcomes in patients with advanced melanoma who discontinued treatment with nivolumab and ipilimumab because of adverse events: a pooled analysis of randomized phase II and III trials. J Clin Oncol 2017, 35:3807–3814
9. Yu H, Boyle TA, Zhou C, Rimm DL, Hirsch FR: PD-L1 expression in lung cancer. J Thorac Oncol 2016, 11:964–975
10. Buttner R, Gosney JR, Skov BG, Adam J, Motoi N, Bloom KJ, Dietel M, Longshore JW, Lopez-Rios F, Penault-Llorca F, Viale G, Wotherspoon AC, Kerr KM, Tsao MS: Programmed death-ligand 1 immunohistochemistry testing: a review of analytical assays and clinical implementation in non-small-cell lung cancer. J Clin Oncol 2017, 35:3867–3876
11. Hofman P: PD-L1 immunohistochemistry for non-small cell lung carcinoma: which strategy should be adopted? Expert Rev Mol Diagn 2017, 17:1097–1108
12. Ilie M, Hofman V, Dietel M, Soria JC, Hofman P: Assessment of the PD-L1 status by immunohistochemistry: challenges and perspectives for therapeutic strategies in lung cancer patients. Virchows Arch 2016, 468:511–525
13. Patel SP, Kurzrock R: PD-L1 expression as a predictive biomarker in cancer immunotherapy. Mol Cancer Ther 2015, 14:847–856
14. Shukuya T, Carbone DP: Predictive markers for the efficacy of anti-PD-1/PD-L1 antibodies in lung cancer. J Thorac Oncol 2016, 11:976–988
15. Ward R, Meagher A, Tomlinson I, O'Connor T, Norrie M, Wu R, Hawkins N: Microsatellite instability and the clinicopathological features of sporadic colorectal cancer. Gut 2001, 48:821–829
16. Boussios S, Ozturk MA, Moschetta M, Karathanasi A, Zakynthinakis-Kyriakou N, Katsanos KH, Christodoulou DK, Pavlidis N: The developing story of predictive biomarkers in colorectal cancer. J Pers Med 2019, 9:E12

17. Hellmann MD, Rizvi NA, Goldman JW, Gettinger SN, Borghaei H, Brahmer JR, Ready NE, Gerber DE, Chow LQ, Juergens RA, Shepherd FA, Laurie SA, Geese WJ, Agrawal S, Young TC, Li X, Antonia SJ: Nivolumab plus ipilimumab as first-line treatment for advanced non-small-cell lung cancer (CheckMate 012): results of an open-label, phase 1, multicohort study. Lancet Oncol 2017, 18:31−41
18. Carbone DP, Reck M, Paz-Ares L, Creelan B, Horn L, Steins M, Felip E, van den Heuvel MM, Ciuleanu TE, Badin F, Ready N, Hiltermann TJN, Nair S, Juergens R, Peters S, Minenza E, Wrangle JM, Rodriguez-Abreu D, Borghaei H, Blumenschein GR Jr, Villaruz LC, Havel L, Krejci J, Corral Jaime J, Chang H, Geese WJ, Bhagavatheeswaran P, Chen AC, Socinski MA, CheckMate I: First-line nivolumab in stage IV or recurrent non-small-cell lung cancer. N Engl J Med 2017, 376:2415−2426
19. Hellmann MD, Ciuleanu TE, Pluzanski A, Lee JS, Otterson GA, Audigier-Valette C, Minenza E, Linardou H, Burgers S, Salman P, Borghaei H, Ramalingam SS, Brahmer J, Reck M, O'Byrne KJ, Geese WJ, Green G, Chang H, Szustakowski J, Bhagavatheeswaran P, Healey D, Fu Y, Nathan F, Paz-Ares L: Nivolumab plus ipilimumab in lung cancer with a high tumor mutational burden. N Engl J Med 2018, 378:2093−2104
20. Hellmann MD, Nathanson T, Rizvi H, Creelan BC, Sanchez-Vega F, Ahuja A, Ni A, Novik JB, Mangarin LMB, Abu-Akeel M, Liu C, Sauter JL, Rekhtman N, Chang E, Callahan MK, Chaft JE, Voss MH, Tenet M, Li XM, Covello K, Renninger A, Vitazka P, Geese WJ, Borghaei H, Rudin CM, Antonia SJ, Swanton C, Hammerbacher J, Merghoub T, McGranahan N, Snyder A, Wolchok JD: Genomic features of response to combination immunotherapy in patients with advanced non-small-cell lung cancer. Cancer Cell 2018, 33:843−852.e844
21. Heeke S, Benzaquen J, Long-Mira E, Audelan B, Lespinet V, Bordone O, Lalvee S, Zahaf K, Poudenx M, Humbert O, Montaudie H, Dugourd PM, Chassang M, Passeron T, Delingette H, Marquette CH, Hofman V, Stenzinger A, Ilie M, Hofman P: In-house implementation of tumor mutational burden testing to predict durable clinical benefit in non-small cell lung cancer and melanoma patients. Cancers (Basel) 2019, 11:E1271
22. Alborelli I, Leonards K, Rothschild SI, Leuenberger LP, Savic Prince S, Mertz KD, Poechtrager S, Buess M, Zippelius A, Laubli H, Haegele J, Tolnay M, Bubendorf L, Quagliata L, Jermann P: Tumor mutational burden assessed by targeted NGS predicts clinical benefit from immune checkpoint inhibitors in non-small cell lung cancer. J Pathol 2020, 250:19−29
23. Rizvi NA, Hellmann MD, Snyder A, Kvistborg P, Makarov V, Havel JJ, Lee W, Yuan J, Wong P, Ho TS, Miller ML, Rekhtman N, Moreira AL, Ibrahim F, Bruggeman C, Gasmi B, Zappasodi R, Maeda Y, Sander C, Garon EB, Merghoub T, Wolchok JD, Schumacher TN, Chan TA: Cancer immunology: mutational landscape determines sensitivity to PD-1 blockade in non-small cell lung cancer. Science 2015, 348:124−128
24. Schumacher TN, Schreiber RD: Neoantigens in cancer immunotherapy. Science 2015, 348:69−74
25. Samstein RM, Lee CH, Shoushtari AN, Hellmann MD, Shen R, Janjigian YY, et al: Tumor mutational load predicts survival after immunotherapy across multiple cancer types. Nat Genet 2019, 51:202−206
26. Alexandrov LB, Nik-Zainal S, Wedge DC, Aparicio SA, Behjati S, Biankin AV, et al: Signatures of mutational processes in human cancer. Nature 2013, 500:415−421
27. Alexandrov LB, Ju YS, Haase K, Van Loo P, Martincorena I, Nik-Zainal S, Totoki Y, Fujimoto A, Nakagawa H, Shibata T, Campbell PJ, Vineis P, Phillips DH, Stratton MR: Mutational signatures associated with tobacco smoking in human cancer. Science 2016, 354:618−622
28. Brash DE, Rudolph JA, Simon JA, Lin A, McKenna GJ, Baden HP, Halperin AJ, Ponten J: A role for sunlight in skin cancer: UV-induced p53 mutations in squamous cell carcinoma. Proc Natl Acad Sci U S A 1991, 88:10124−10128
29. Chalmers ZR, Connelly CF, Fabrizio D, Gay L, Ali SM, Ennis R, Schrock A, Campbell B, Shlien A, Chmielecki J, Huang F, He Y, Sun J, Tabori U, Kennedy M, Lieber DS, Roels S, White J, Otto GA, Ross JS, Garraway L, Miller VA, Stephens PJ, Frampton GM: Analysis of 100,000 human cancer genomes reveals the landscape of tumor mutational burden. Genome Med 2017, 9:34
30. Mensenkamp AR, Vogelaar IP, van Zelst-Stams WA, Goossens M, Ouchene H, Hendriks-Cornelissen SJ, Kwint MP, Hoogerbrugge N, Nagtegaal ID, Ligtenberg MJ: Somatic mutations in MLH1 and MSH2 are a frequent cause of mismatch-repair deficiency in Lynch syndrome-like tumors. Gastroenterology 2014, 146:643−646.e648
31. Pursell ZF, Isoz I, Lundstrom EB, Johansson E, Kunkel TA: Yeast DNA polymerase epsilon participates in leading-strand DNA replication. Science 2007, 317:127−130
32. Vanderwalde A, Spetzler D, Xiao N, Gatalica Z, Marshall J: Microsatellite instability status determined by next-generation sequencing and compared with PD-L1 and tumor mutational burden in 11,348 patients. Cancer Med 2018, 7:746−756
33. Kohsaka S, Petronczki M, Solca F, Maemondo M: Tumor clonality and resistance mechanisms in EGFR mutation-positive non-small-cell lung cancer: implications for therapeutic sequencing. Future Oncol 2019, 15:637−652
34. Manzano JL, Layos L, Buges C, de Los Llanos Gil M, Vila L, Martinez-Balibrea E, Martinez-Cardus A: Resistant mechanisms to BRAF inhibitors in melanoma. Ann Transl Med 2016, 4:237
35. Kalbasi A, Ribas A: Tumour-intrinsic resistance to immune checkpoint blockade. Nat Rev Immunol 2020, 20:25−39
36. Neveling K, Feenstra I, Gilissen C, Hoefsloot LH, Kamsteeg EJ, Mensenkamp AR, Rodenburg RJ, Yntema HG, Spruijt L, Vermeer S, Rinne T, van Gassen KL, Bodmer D, Lugtenberg D, de Reuver R, Buijsman W, Derks RC, Wieskamp N, van den Heuvel B, Ligtenberg MJ, Kremer H, Koolen DA, van de Warrenburg BP, Cremers FP, Marcelis CL, Smeitink JA, Wortmann SB, van Zelst-Stams WA, Veltman JA, Brunner HG, Scheffer H, Nelen MR: A post-hoc comparison of the utility of sanger sequencing and exome sequencing for the diagnosis of heterogeneous diseases. Hum Mutat 2013, 34:1721−1726
37. Eijkelenboom A, Tops BBJ, van den Berg A, van den Brule AJC, Dinjens WNM, Dubbink HJ, Ter Elst A, Geurts-Giele WRR, Groenen P, Groenendijk FH, Heideman DAM, Huibers MMH, Huijsmans CJJ, Jeuken JWM, van Kempen LC, Korpershoek E, Kroeze LI, de Leng WWJ, van Noesel CJM, Speel EM, Vogel MJ, van Wezel T, Nederlof PM, Schuuring E, Ligtenberg MJL: Recommendations for the clinical interpretation and reporting of copy number gains using gene panel NGS analysis in routine diagnostics. Virchows Arch 2019, 474:673−680
38. Eijkelenboom A, Kamping EJ, Kastner-van Raaij AW, Hendriks-Cornelissen SJ, Neveling K, Kuiper RP, Hoischen A, Nelen MR, Ligtenberg MJ, Tops BB: Reliable next-generation sequencing of formalin-fixed, paraffin-embedded tissue using single molecule tags. J Mol Diagn 2016, 18:851−863
39. Steeghs EMP, Kroeze LI, Tops BBJ, van Kempen LC, ter Elst A, Kastner-van Raaij AWM, Hendriks-Cornelissen SJB, Hermsen MJW, Jansen EAM, Nederlof PM, Schuuring E, Ligtenberg MJL, Eijkelenboom A: Comprehensive routine diagnostic screening to identify predictive mutations, gene amplifications, and microsatellite instability in FFPE tumor material. BMC Cancer 2020, 20:291
40. Salipante SJ, Scroggins SM, Hampel HL, Turner EH, Pritchard CC: Microsatellite instability detection by next generation sequencing. Clin Chem 2014, 60:1192−1199
41. Rosenthal R, McGranahan N, Herrero J, Taylor BS, Swanton C: DeconstructSigs: delineating mutational processes in single tumors distinguishes DNA repair deficiencies and patterns of carcinoma evolution. Genome Biol 2016, 17:31
42. Kazdal D, Endris V, Allgauer M, Kriegsmann M, Leichsenring J, Volckmar AL, Harms A, Kirchner M, Kriegsmann K, Neumann O,

Brandt R, Talla SB, Rempel E, Ploeger C, von Winterfeld M, Christopoulos P, Merino DM, Stewart M, Allen J, Bischoff H, Meister M, Muley T, Herth F, Penzel R, Warth A, Winter H, Frohling S, Peters S, Swanton C, Thomas M, Schirmacher P, Budczies J, Stenzinger A: Spatial and temporal heterogeneity of panel-based tumor mutational burden in pulmonary adenocarcinoma: separating biology from technical artifacts. J Thorac Oncol 2019, 14:1935−1947

43. Allgauer M, Budczies J, Christopoulos P, Endris V, Lier A, Rempel E, Volckmar AL, Kirchner M, von Winterfeld M, Leichsenring J, Neumann O, Frohling S, Penzel R, Thomas M, Schirmacher P, Stenzinger A: Implementing tumor mutational burden (TMB) analysis in routine diagnostics: a primer for molecular pathologists and clinicians. Transl Lung Cancer Res 2018, 7:703−715
44. Buttner R, Longshore JW, Lopez-Rios F, Merkelbach-Bruse S, Normanno N, Rouleau E, Penault-Llorca F: Implementing TMB measurement in clinical practice: considerations on assay requirements. ESMO Open 2019, 4:e000442
45. Stenzinger A, Allen JD, Maas J, Stewart MD, Merino DM, Wempe MM, Dietel M: Tumor mutational burden standardization initiatives: recommendations for consistent tumor mutational burden assessment in clinical samples to guide immunotherapy treatment decisions. Genes Chromosomes Cancer 2019, 58:578−588
46. Van Hoeck A, Tjoonk NH, van Boxtel R, Cuppen E: Portrait of a cancer: mutational signature analyses for cancer diagnostics. BMC Cancer 2019, 19:457
47. Rebhandl S, Huemer M, Greil R, Geisberger R: AID/APOBEC deaminases and cancer. Oncoscience 2015, 2:320−333
48. Chen H, Chong W, Teng C, Yao Y, Wang X, Li X: The immune response-related mutational signatures and driver genes in non-small-cell lung cancer. Cancer Sci 2019, 110:2348−2356
49. Wang S, Jia M, He Z, Liu XS: APOBEC3B and APOBEC mutational signature as potential predictive markers for immunotherapy response in non-small cell lung cancer. Oncogene 2018, 37: 3924−3936
50. Rizvi H, Sanchez-Vega F, La K, Chatila W, Jonsson P, Halpenny D, Plodkowski A, Long N, Sauter JL, Rekhtman N, Hollmann T, Schalper KA, Gainor JF, Shen R, Ni A, Arbour KC, Merghoub T, Wolchok J, Snyder A, Chaft JE, Kris MG, Rudin CM, Socci ND, Berger MF, Taylor BS, Zehir A, Solit DB, Arcila ME, Ladanyi M, Riely GJ, Schultz N, Hellmann MD: Molecular determinants of response to anti-programmed cell death (PD)-1 and anti-programmed death-ligand 1 (PD-L1) blockade in patients with non-small-cell lung cancer profiled with targeted next-generation sequencing. J Clin Oncol 2018, 36:633−641
51. Prelaj A, Tay R, Ferrara R, Chaput N, Besse B, Califano R: Predictive biomarkers of response for immune checkpoint inhibitors in non-small-cell lung cancer. Eur J Cancer 2019, 106:144−159
52. Yarchoan M, Hopkins A, Jaffee EM: Tumor mutational burden and response rate to PD-1 inhibition. N Engl J Med 2017, 377: 2500−2501